

RESEARCH ARTICLE

A STOICHIOMETRIC MODEL OF TWO PRODUCERS AND ONE CONSUMER

LAURENCE HAO-RAN LIN^{a*◇}, BRUCE PECKHAM^{a**}, HARLAN STECH^{a†},
and JOHN PASTOR^{b‡}

^a*Department of Mathematics and Statistics, University of Minnesota, Duluth MN 55812;
Dept. Fax: 218-726-8399;*

^b*Department of Biology, University of Minnesota, Duluth MN 55812; Dept. Fax: 218-726-8142;*

*Email: linx0275@d.umn.edu, Contact Phone: 218-349-3782

**Email: bpeckham@d.umn.edu, Office Phone: 218-726-6188

†Email: hstech@d.umn.edu, Office Phone: 218-726-8272

‡Email: jpastor@d.umn.edu, Office Phone: 218-726-7001

(v1.0 released August 2008)

In this paper, we consider a stoichiometric population model of two producers and one consumer. It is a generalization of the Rosenzweig-MacArthur population growth model, which is a one-producer, one-consumer population model without stoichiometry. The generalization involves two steps: 1) adding a second producer which competes with the first, and 2) introducing stoichiometry into the system. Both generalizations introduce additional equilibria and bifurcations to those of the Rosenzweig-MacArthur model without stoichiometry.

The primary focus of this paper is to study the equilibria and bifurcations of the two-producer, one-consumer model with stoichiometry. The nutrient cycle in this model is closed. The primary parameters are the growth rates of both producers. A secondary parameter is the total nutrient in the system. Depending on the parameters the possible equilibria are: no-life, one-producer, coexistence of both producers, the consumer coexisting with either producer, and the consumer coexisting with both producers. Limit cycles exist in the latter three coexistence combinations. Bifurcation diagrams along with corresponding representative time series summarize the behaviors observed for this model.

Keywords: Stoichiometry, Producer-Consumer Model, Second Producer, Coexistence

1. Introduction

A population is the collection of inter-breeding organisms of a particular species. Mathematical population models follow the size of interacting populations over time. Such models are fundamental in biology and ecology. A producer-consumer (prey-predator) population model studies the populations of two species which interact in a specific way. A variety of producer-consumer models has been developed and studied over the last century, usually with a single currency, such as biomass, for each population. More recently, stoichiometry, which can be thought as tracking food quality as well as quantity, has been introduced into population models [1, 5, 6, 8, 12–15].

◇Corresponding author. Email: linx0275@d.umn.edu, laurenl@vt.edu

Every organism has its own ratios of nutrients in its body, and those ratios are called “stoichiometric ratios.” Stoichiometric ratios are very specific for most animals, but plants have been observed to have a wide range of values [12]. In this paper a single stoichiometric ratio, N:C, represented by an unnamed nutrient (N) and carbon (C) is tracked. Food that has a very low stoichiometric ratio compared to the consumer’s ratio is not of as much benefit to consumer growth. Stoichiometric models, especially those with a closed nutrient cycle, tend to exhibit a “paradox of enrichment”, a phenomenon in which the population of the consumer declines in response to an increase in the population of the producer [4, 8, 14].

In 1963, Rosenzweig and MacArthur [11] spresented a geometric analysis of producer growth and consumer response. It has become one of the classic producer-consumer population models with a single currency, carbon. Formulas (1) are the traditional realization of the Rosenzweig-MacArthur model, using logistic producer growth and Michaelis-Menten consumer response with food saturation.

$$\left\{ \begin{array}{l} \frac{dP}{dt} = \alpha P - \lambda P^2 - f(P)C \\ \frac{dC}{dt} = e f(P)C - dC \\ f(P) = \frac{\beta P}{\chi + P} \end{array} \right. \quad (1)$$

α is the maximal per-capita growth rate of producer in the absence of predation.

λ is the producer self-limitation coefficient.

e is the efficiency of turning predated food into consumer’s biomass.

d is the per-capita death rate of consumer.

$f(P)$ is a Holling Type II or Michaelis-Menten function that describes consumers’ food saturation.

β is the maximal death rate per encounter of producer due to predation.

χ is the half-saturation constant for the Michaelis-Menten function.

A standard parameter to vary in (1) is the producer growth rate α . For low α the ecosystem is a producer monoculture system because there is not enough food to maintain the consumer. Increasing α sufficiently to pass a transcritical bifurcation value allows both producer and consumer to stable coexist. Further increase in α results in a destabilization of the coexistence equilibrium in a Hopf bifurcation, accompanied by the birth of an attracting limit cycle. The amplitude of the cycle grows with continuing increase in α , but no further bifurcations are observed [16].

In 2000, Loladze, Kuang and Elser (LKE) [8] introduced a producer-consumer population model with stoichiometry, which has become a basis of comparison for most subsequent stoichiometric models. Their model was based on the Rosenzweig-MacArthur model and exhibits the “paradox of enrichment” [4, 14]. The equations for the LKE model are:

$$\begin{cases} \frac{dP}{dt} = \alpha P \left(1 - \frac{P}{\min(K, (N_T - \theta C)/q)}\right) - f(P)C \\ \frac{dC}{dt} = \hat{e} \min\left(1, \frac{(N_T - \theta C)/P}{\theta}\right) f(P)C - dC \end{cases} \quad (2)$$

α is the maximal per-capita growth rate of producer in the absence of predation.
 K is the high nutrient level carrying capacity of producer with the absence of consumer.

\hat{e} is the maximal production efficiency.

d is the per-capita death rate of consumer.

N_T is total amount of nutrient in the model.

θ is a (fixed) stoichiometric ratio of the consumer class.

q is the minimum stoichiometric ratio of producer.

$f(P)$ is a function to describe consumer's response to food. This is typically a Michaelis-Menten (Holling type II), as in (1).

The total nutrient, N_T is assumed to be fixed, consistent with a closed nutrient system. There are two stoichiometric influences, the producer's carrying capacity, $\min(K, (N_T - \theta C)/q)$, and the consumer's biomass conversion efficiency, $\min(1, \frac{(N_T - \theta C)/P}{\theta})$. If the two stoichiometric "min" functions were each replaced with the first arguments in the respective min functions, the system would revert to the nonstoichiometric Rosenzweig-MacArthur model, equivalent to equation (1). The equivalence is seen by replacing the first equation in (1) with $\frac{dP}{dt} = \alpha P \left(1 - \frac{P}{K}\right) - f(P)C$. Varying K with this replacement for a specific choice of a scenery parameter results in the same qualitative bifurcation sequence as just described above for varying α in (1) [16]. With the stoichiometric terms, however, varying K results in new bifurcations. The sequence mimics the bifurcations described above for the Rosenzweig-MacArthur model through the Hopf bifurcation, but continued increase in K now results in the destruction of the limit cycle due to a saddle-node birth of equilibria on the limit cycle. The stable node born in the bifurcation replaces the limit cycle as the attractor. Continued increase in K exhibits the paradox of enrichment. The consumer values of the equilibrium decrease until a transcritical bifurcation value after which the consumer can no longer exist. The nutrient is distributed in the large producer population, that is of insufficient quality for the consumer to survive.

A natural way to generalize a stoichiometric producer-consumer model is to allow for more species. For example, a variety of grazing species in a corn field would require a model of one producer and multiple consumers [9]. Yet an ecosystem of a garden of various flowers might be a model of multiple producers and one consumer (a certain type of insect). In Pastor and Cohen [10] a model of one consumer, two producers, and a single currency (no stoichiometry) was addressed. The focus of the model was to determine the criteria of coexistence in terms of plants' growth rates in open and closed environments. An open environment means there are nutrient inputs from and exports to the surrounding environments for some components. A closed environment corresponds to those having a fixed total amount of nutrient cycling through the components in the model. In this paper we present a theoretical study of a two-producer, single-consumer system. Our model is open for carbon, but closed for its nutrient.

It can be thought of as a generalization of the Pastor-Cohen model, now with stoichiometry. Alternatively, it can be thought of as a generalization of the LKE model, with a second producer. Our stoichiometric assumptions, however, differ in certain aspects from the LKE assumptions.

There are many interesting questions associated with a model of two producers and one consumer with stoichiometry: (i) Under what conditions can all three species stable coexist? In equilibrium? As a periodic limit cycle? Or some attractors? (ii) How does the producer competition affect coexistence? What about differences in producer growth? (iii) What new transitions are possible when a system moves from one producer to two producers? This paper includes a bifurcation study – largely numerical – of the model of two producers and one consumer with stoichiometry, focusing on the questions above.

Much of the work presented in this paper was performed for the master's thesis of the first author [7].

2. Model Construction

This model contains two populations of producer and a single population of consumer. Since this is a stoichiometric model, both quality and quantity of producer and consumer are measured. We choose to keep track of carbon as a measure of quantity, and nutrient (later changed to the nutrient-to-carbon ratio) as a measure of quality. This leads to six density variables (g): $P_1, P_2, C, N_1, N_2, N_C$. We also keep track of the nutrient in the sediment, $M(g)$. Variables of the model are summarized in table 1. As we describe below, a sediment class for the carbon is not necessary. The model we will actually study is reduced from these seven variables to five by assuming a fixed amount of total nutrient, and a fixed stoichiometric ratio $q = N_C/C$ for the consumer. Details are provided below. Figure 1 illustrates the flow of carbon and cycling of a nutrient in this model.

The equations for our model are given below in equation (3). We now describe the assumptions which lead to the equations.

$$\left\{ \begin{array}{l} \frac{dP_1}{dt} = (b_1 - \lambda_{11}P_1 - \lambda_{12}P_2)^+ P_1 - d_{p1}P_1 - \frac{P_1}{P_1+P_2} \frac{\alpha(P_1+P_2)}{h+(P_1+P_2)} C \\ \frac{dP_2}{dt} = (b_2 - \lambda_{21}P_1 - \lambda_{22}P_2)^+ P_2 - d_{p2}P_2 - \frac{P_2}{P_1+P_2} \frac{\alpha(P_1+P_2)}{h+(P_1+P_2)} C \\ \frac{dC}{dt} = \min(\gamma, \frac{1}{q} \frac{N_1+N_2}{P_1+P_2}) \frac{\alpha(P_1+P_2)}{h+(P_1+P_2)} C - d_c C \\ \frac{dN_1}{dt} = (N_T - N_c - N_1 - N_2) \beta_1 (b_1 - \lambda_{11}P_1 - \lambda_{12}P_2)^+ P_1 - \frac{P_1}{P_1+P_2} \frac{\alpha(P_1+P_2)}{h+(P_1+P_2)} C \frac{N_1}{P_1} - d_{p1}N_1 \\ \frac{dN_2}{dt} = (N_T - N_c - N_1 - N_2) \beta_2 (b_2 - \lambda_{21}P_1 - \lambda_{22}P_2)^+ P_2 - \frac{P_2}{P_1+P_2} \frac{\alpha(P_1+P_2)}{h+(P_1+P_2)} C \frac{N_2}{P_2} - d_{p2}N_2 \end{array} \right. \quad (3)$$

The biomass (carbon) of the producer is assumed to follow logistic growth. Note that we have chosen to make the producer growth independent of the

nutrient. This independence assumption simplifies the analysis and focuses the role of stoichiometry on the food quality of the consumer. As is necessary in stoichiometric models, the death terms are separated from the (logistic) growth terms in this model. This is the reason for the use of the “positive part” function, $()^+$, in the first two equations of (3). Producer respiration is modeled as a fixed fraction of the carbon fixation through the photosynthesis. That is, “growth” is interpreted as “net growth”. We assume that the rates of litter decomposition and nutrient mineralization are independent of sediment nutrient concentration. Thus, there is no need to include a sediment carbon compartment in the model. Mortality is considered as an exit of carbon from the system. (See figure 1(a).)

This is a closed nutrient model: The amount of nutrient in the system is fixed. There are no external nutrient input and output in any components. In other words, all nutrients are cycling within the model. Let N_T be the total nutrient in system. Then, by this assumption, the amount of mineralized nutrient, $M = N_T - N_c - N_1 - N_2$.

Lotka-Volterra competition is assumed between the two producers. The product of the competition coefficients $\lambda_{12}\lambda_{21}$ is assumed to be always less than the product of the self-limitation coefficients $\lambda_{11}\lambda_{22}$ [2]. Otherwise, the two producers could not coexist even in the absence of the consumer.

The predation of both producers (consumer response) is assumed to follow a Michaelis-Menten function. Both producers are food for the consumer, which favors non-preferentially; the probabilities of producer P_1 and P_2 being eaten are assumed to be $\frac{P_1}{P_1+P_2}$ and $\frac{P_2}{P_1+P_2}$, respectively. That is, the producers are consumed in proportion to their relative abundance.

The consumer gains biomass through predation. The maximum conversion efficiency is assumed to be a constant, γ , without stoichiometry. However, it becomes a minimum function of γ and $\frac{N_1+N_2}{q(P_1+P_2)}$, the ratio of the aggregate food source’s stoichiometry to the consumer’s stoichiometry. When the food source contains sufficient nutrient to support the maximum conversion efficiency γ , then the rate γ is achieved. Otherwise, the conversion efficiency is reduced to $\frac{N_1+N_2}{q(P_1+P_2)}$, reflecting the maximum rate at which nutrient can be supplied to build structural consumer biomass. Consumer death is assumed to be proportional to its population size.

The producer gains nutrient via uptake from the mineralized nutrient, and loses nutrient due to predation and mortality. The nutrient uptake rate in this model is proportional to the mineralized nutrient $M = N_T - N_c - N_1 - N_2$. In contrast to other stoichiometric models, nutrient uptake is also assumed to be proportional to producer growth. This assumption appears to be realistic for terrestrial plants [3]. Where nutrient uptake is proportional to plant transpiration and, of course, would be required of producers that maintain a constant $N : C$ ratio. Nutrient is transferred from producer to consumer via predation, and returned to the nutrient pool when either a producer or the consumer dies. The nutrient uptake coefficients β_1 and β_2 are assumed to be constant.

To reduce the complexity of formulas (3), we use $Q_i = \frac{N_i}{P_i}$, $i = 1, 2$ to replace N_1 and N_2 . Then calculating the derivatives of Q_1 and Q_2 , we get the “stoichiometric form” of the system:

$$\left\{ \begin{array}{l} \frac{dP_1}{dt} = ((b_1 - \lambda_{11}P_1 - \lambda_{12}P_2)^+ - d_{p_1} - \frac{\alpha C}{h+(P_1+P_2)})P_1 \\ \frac{dP_2}{dt} = ((b_2 - \lambda_{21}P_1 - \lambda_{22}P_2)^+ - d_{p_2} - \frac{\alpha C}{h+(P_1+P_2)})P_2 \\ \frac{dC}{dt} = (\min(\gamma, \frac{1}{q} \frac{P_1Q_1+P_2Q_2}{P_1+P_2}) \frac{\alpha(P_1+P_2)}{h+(P_1+P_2)} - d_c)C \\ \frac{dQ_1}{dt} = ((N_T - qC - Q_1P_1 - Q_2P_2)\beta_1 - Q_1)(b_1 - \lambda_{11}P_1 - \lambda_{22}P_2)^+ \\ \frac{dQ_2}{dt} = ((N_T - qC - Q_1P_1 - Q_2P_2)\beta_2 - Q_2)(b_2 - \lambda_{21}P_1 - \lambda_{22}P_2)^+ \end{array} \right. \quad (4)$$

Note that $\frac{dC}{dt}$ is not defined if both P_1 and P_2 are zero. It can, however, be continuously extended to $P_1 = P_2 = 0$ by $\frac{dC}{dt} = -d_C C$.

For our numerical investigations, we fixed the following parameters, representing two nearly identical producer species (differing only in maximal per-capita growth rates) and a nutrient-rich consumer.

Self-limiting coefficients: $\lambda_{11} = \lambda_{22} = 0.5\text{g}^{-1}\text{month}^{-1}$

Interference coefficients: $\lambda_{12} = \lambda_{21} = 0.2\text{g}^{-1}\text{month}^{-1}$

Producer per-capita natural death rates: $d_{P_1} = d_{P_2} = 0.05\text{month}^{-1}$

Consumer per-capita death rate: $d_c = 0.17\text{month}^{-1}$

Consumer stoichiometric ratio: $q = 0.05$

Efficient conversation ratio: $\gamma = 0.1$

Maximal and half-saturation coefficients in the predation function, f : $\alpha = 2.75\text{month}^{-1}$ and $h = 0.75\text{g}$,

Nutrient uptake constants $\beta_1 = \beta_2 = 0.3\text{g}^{-1}$.

As our goal is to determine as in [8] the effects of system enrichment under a fixed nutrient budget, the remaining parameters $b_1\text{month}^{-1}$, $b_2\text{month}^{-1}$, and $N_T\text{g}$ are varied in our numerical experiments. All rate constants are dependent on the units selected to measure biomass and nutrient densities. We have selected to not normalize the equations, as this somewhat obscures the interpretation of our numerical findings. The selected parameter set is motivated by a hypothetical grassland-herbivore system measured at a weekly time scale.

3. One-Producer, One-Consumer Model

In order to more easily understand the model (4), we first consider the special case where there is a single producer in the system. This one-producer, one-consumer model is similar to the LKE model [8], but with different nutrient uptake assumptions. We set $P_2 = 0$ and ignore Q_2 to obtain:

$$\left\{ \begin{array}{l} \frac{dP_1}{dt} = (b_1 - \lambda_{11}P_1 - d_{P_1} - \frac{\alpha C}{h+P_1})P_1 \\ \frac{dC}{dt} = (\min(\gamma, \frac{Q_1}{q}) \frac{\alpha P_1}{h+P_1} - d_c)C \\ \frac{dQ_1}{dt} = ((N_T - qC - Q_1P_1)\beta_1 - Q_1)(b_1 - \lambda_{11}P_1) \end{array} \right. \quad (5)$$

The positive part function from (4) has been eliminated as a consequence of the following Proposition.

Proposition 3.1: *The following inequalities describe an invariant region of model (5): $0 \leq P_1 \leq \frac{b_1}{\lambda_{11}}$, $0 \leq C \leq \frac{N}{q}$, $0 \leq Q_1 \leq N_T\beta$, and $(N_T - qC - Q_1P_1) \geq 0$.*

Proof: The proof, which is standard for related models in the literature, follows by showing that all solutions which start on the boundary of the region will stay on the boundary or go to the interior of the region. See [7] for details.

□

Equilibria

We calculate the system equilibria, with the variables listed in the order: (P_1, C, Q_1) .

The no-life equilibrium (O): $(0, 0, N_T\beta_1)$, where neither producer nor consumer exist, but the (irrelevant) producer stoichiometric ratio is not necessarily zero.

The monoculture equilibrium (P_1) : $(\frac{b_1 - d_{p_1}}{\lambda_{11}}, 0, \frac{N_T\lambda_{11}\beta_1}{\lambda_{11} + (b_1 - d_{p_1})\beta_1})$. In the absence of consumers, the population of producers follows the logistic growth and approaches its carrying capacity $\frac{b_1 - d_{p_1}}{\lambda_{11}}$ over time.

The coexistence equilibrium (P_1C) : There are two cases designated by H and L. In case H (denoting high food quality), the biomass conversion efficiency is $\min(\gamma, \frac{Q_1}{q}) = \gamma$. The conversion efficiency is $\min(\gamma, \frac{Q_1}{q}) = \frac{Q_1}{q}$ in the low food quality case L. We use subscripts to denote the cases.

For case H, the coexistence equilibrium $(P_1C)_H$ is $(\frac{d_c h}{\alpha\gamma - d_c}, \frac{h\gamma(b_1 - d_{p_1})}{\alpha\gamma - d_c} - \frac{\gamma d_c \lambda_{11} h^2}{(\alpha\gamma - d_c)^2}, \frac{\beta(N_T(\alpha\gamma - d_c) - hq\gamma(b_1 - d_{p_1}) + \frac{k\gamma q d_c h^2}{\alpha\gamma - d_c})}{\alpha\gamma - d_c(h\beta_1 - 1)})$. Note that, due to the consumption by consumers, the producer equilibrium level is independent of the growth rate b_1 .

For the case L, the coexistence equilibrium, $(P_1C)_L$ is more complicated. By setting the right hand sides of (5) to zero, solving in the third equation for Q_1 , solving in the second equation for C , and substituting these solutions into the first equation, it can be shown that the equilibria with nonzero P_1 and C must satisfy the following cubic in P_1 .

$$(P_1)^3 c_3 + (P_1)^2 c_2 + (P_1) c_1 + c_0 = 0, \quad (6)$$

where

$$\begin{aligned} c_3 &= -\lambda_{11} \\ c_2 &= b_1 - d_{p_1} + d_c - h\lambda_{11} \\ c_1 &= (b_1 - d_{p_1} + d_c)h - \frac{N_T\alpha}{q} + \frac{d_c}{\beta_1} \\ c_0 &= \frac{hd_c}{\beta_1} \end{aligned}$$

Thus, there can be up to three $(P_1C)_L$ solutions. Along with one possible $(P_1C)_H$

solution, there could exist up to four coexistence equilibria. Fewer are actually realized, however, since the biologically meaningful coexistence solutions must also have positive populations, and satisfy the “consistency condition”: $\frac{Q_1}{q} \geq \gamma$ for $(P_1C)_H$ solutions, and $\frac{Q_1}{q} \leq \gamma$ for $(P_1C)_L$ solutions.

Bifurcations with varying b_1 (maximal per-capita producer productivity) and N_T (total system nutrient) fixed

We provide representative bifurcation diagrams, varying b_1 , in figure 2. The total nutrient N_T is fixed at a relatively low value of 0.1. To illustrate the interplay between biologically meaningful and biologically extraneous equilibria, we plot $\frac{Q_1}{q}$ at the coexistence equilibria $(P_1C)_H$ and $(P_1C)_L$ against b_1 in figure 2(a). The portion of the cubic red curve representing the case L equilibria is biologically meaningful only when the curve is below $\gamma = 0.1$. Conversely, the portion of the slanted blue line representing the case H equilibria is biologically meaningful only when the curve is above γ . The dashed blue segment in region C represents the repelling equilibrium, while the two thin solid lines in region C represent the range of realized $\frac{Q_1}{q}$ along the attracting periodic orbit. The bold curves indicate the biomass conversion efficiency on the attractor: γ at the case H equilibrium in region B, γ throughout most of region C — as long as the minimum value of $\frac{Q_1}{q}$ along the periodic orbit stays above γ , a range of values between γ and the minimum realized $\frac{Q_1}{q}$ on the periodic orbit at the right hand part of region C, and at $\frac{Q_1}{q}$ for the case L equilibrium in regions D through E., solid to attracting, and dashed to unstable. The orange curve in region C indicates the over-time meanvalues on limit cycles. Bifurcations between adjacent regions are described in table 2. Red corresponds to case L, blue to case H

Figures 2(b), 2(c), and 2(d) are more traditional bifurcation diagrams with a fixed $N_T = 0.1$. They correspond to figure 2(a). Bifurcations between regions are indicated on the figure, and identified as well in the chart for the two-parameter plane bifurcations presented in the next paragraph.

Bifurcations with varying b_1 and N_T

To better place the one-parameter bifurcation diagrams in of figure 2 in context, we show a two-parameter bifurcation diagram in b_1 and N_T in figure 3. Corresponding time series plots are shown in figure 4. The solid curves indicate those bifurcations resulting in a change of attractor; the dashed curves indicate bifurcations which do not change the attractor. In each time series, solutions of P_1 , C , and magnified Q_1 are plotted against time. Table 2 describes the bifurcations between the adjacent regions of (b_1, N_T) parameter space. Note that regions A and F, B and E are connected. Region O ($0 \leq b_1 \leq d_{P_1}$), is too small to be shown in figure 3(a), but is to the left of region A. As a comparison, figure 3(b) shows a bifurcation diagram of the corresponding model without stoichiometry (replacing $\min(\gamma, \frac{N_1+N_2}{q(P_1+P_2)})$ with γ). The non-stoichiometric model is, of course, independent of N_T since the model reverts to a single currency model.

4. The Two-Producer, One-Consumer Model

We turn to an analysis of the full model (4), with both producers, one consumer, and stoichiometry. Much of the analysis parallels that performed in the previous section for a single producer.

Proposition 4.1: *The following inequalities describe an invariant region of model (4): $0 \leq P_1 \leq \frac{b_1}{\lambda_{11}}$, $0 \leq P_2 \leq \frac{b_2}{\lambda_{22}}$, $0 \leq C \leq \frac{N_T}{q}$, $0 \leq Q_1 \leq N_T\beta_1$, $0 \leq Q_2 \leq N_T\beta_2$, and $(N_T - qC - Q_1P_1 - Q_2P_2) \geq 0$.*

Proof: The proof is similar to that of Proposition 3.1. See [7] for details.

□

Equilibria

Similar to the one producer model, we first calculate all possible equilibria, with coordinates listed in the order: (P_1, P_2, C, Q_1, Q_2) . There remain two cases: case H, where $\min(\gamma, \frac{Q_1P_1+Q_2P_2}{q(P_1+P_2)}) = \gamma$, and case L, where $\min(\gamma, \frac{Q_1P_1+Q_2P_2}{q(P_1+P_2)}) = \frac{Q_1P_1+Q_2P_2}{q(P_1+P_2)}$. Note that equilibria with $P_2 = 0$ or $P_1 = 0$ are same as the equilibria in the single-producer-single-consumer model in the previous section. We list these equilibria first. Since Q_i is not ecologically relevant when $P_i = 0$, we denote the corresponding mathematical equilibrium value as being “not applicable” (NA).

- The no-life equilibrium (O): $(0, 0, 0, \text{NA}, \text{NA})$
- The monoculture equilibrium (P_1): $(\frac{b_1-d_{P_1}}{\lambda_{11}}, 0, 0, \frac{N_T\beta_1\lambda_{11}}{\lambda_{11}+(b_1-d_{P_1})\beta_1}, \text{NA})$
- The monoculture equilibrium (P_2): $(0, \frac{b_2-d_{P_2}}{\lambda_{22}}, 0, \text{NA}, \frac{N_T\beta_2\lambda_{22}}{\lambda_{22}+(b_2-d_{P_2})\beta_2})$
- The one-producer coexistence equilibrium (P_1C)_H: $(\frac{d_c h}{\gamma\alpha-d_c}, 0, \frac{\gamma h(b_1-d_{P_1})}{\alpha\gamma-d_c} - \frac{\gamma d_c h^2 \lambda_{11}}{(\alpha\gamma-d_c)^2}, \frac{\beta_1(N_T(\alpha\gamma-d_c)-h q \gamma(b_1-d_{P_1})-\frac{d_c q \gamma h^2 \lambda_{11}}{\alpha\gamma-d_c})}{\alpha\gamma-d_c(h\beta_1-1)}, \text{NA})$.
- The one-producer coexistence equilibrium (P_2C)_H: $(0, \frac{d_c h}{\gamma\alpha-d_c}, \frac{\gamma h(b_2-d_{P_2})}{\alpha\gamma-d_c} - \frac{\gamma d_c h^2 \lambda_{22}}{(\alpha\gamma-d_c)^2}, \text{NA}, \frac{\beta_2(N_T(\alpha\gamma-d_c)-h q \gamma(b_2-d_{P_2})-\frac{d_c q \gamma h^2 \lambda_{22}}{\alpha\gamma-d_c})}{\alpha\gamma-d_c(h\beta_2-1)})$.

The following are new coexistence equilibria, involving both producers, in the two-producer-one-consumer model. Note that the coexistence equilibrium solution in biological meaningful only when the growth terms $(b_1 - \lambda_{12}P_2 - \lambda_{11}P_1)$ and $(b_2 - \lambda_{21}P_1 - \lambda_{22}P_2)$ both are positive.

- The coexistence equilibrium without consumer (P_1P_2):

We set $C = 0$ and assume that all other variables are positive. The equilibrium solution is computed to be $(P_1, P_2, C, Q_1, Q_2) =$

$$(\frac{\lambda_{22}B_1-\lambda_{12}B_2}{S_{prod}}, \frac{\lambda_{11}B_2-\lambda_{21}B_1}{S_{prod}}, 0, \frac{N_T\beta_1S_{prod}}{B_1(\beta_1\lambda_{22}-\beta_2\lambda_{21})+B_2(\beta_2\lambda_{11}-\beta_1\lambda_{12})+S}, \frac{N_T\beta_2S_{prod}}{B_1(\beta_1\lambda_{22}-\beta_2\lambda_{21})+B_2(\beta_2\lambda_{11}-\beta_1\lambda_{12})+S}),$$

where $B_1 = b_1 - d_{P_1}$, $B_2 = b_2 - d_{P_2}$, and $S_{prod} = \lambda_{11}\lambda_{22} - \lambda_{12}\lambda_{21}$

In the absence of the consumer, our model reduces to a Lotka-Volterra competition model. Our simplifying assumption that the producer growth be independent of the stoichiometry renders Q_1 and Q_2 irrelevant. Note that in order to keep the equilibrium value of P_1 and P_2 positive, the product

of self limitation terms, $\lambda_{11}\lambda_{22}$, must be “large” compared to the product of competition coefficients $\lambda_{12}\lambda_{21}$. Note also that if b_1 is sufficiently large, with other parameters being fixed, the equilibrium value of P_2 becomes negative; that is, ecologically, P_2 cannot persist. An analogous statement is true for large b_2 . Consequently, coexistence of both producers requires the two birth rates be relatively close to each other.

- High food quality coexistence equilibrium $(P_1P_2C)_H$:

We assume that $\min(\gamma, \frac{N_1+N_2}{q(P_1+P_2)}) = \gamma$. Note that in order to keep the components of the all-species-coexistence equilibrium positive, the sum of the self-limitations $\lambda_{11} + \lambda_{22}$ is assumed to be larger than the sum of the competition-limitations $\lambda_{12} + \lambda_{21}$.

Assuming all variables are positive, the equilibrium solution is

$$(P_1P_1P_2C, P_2P_1P_2C, C_{P_1P_2C}, \frac{\beta_1(N_T - qC_{P_1P_2C})}{1+\beta_1P_1P_1P_2C+\beta_2P_2P_1P_2C}, \frac{\beta_2(N_T - qC_{P_1P_2C})}{1+\beta_1P_1P_1P_2C+\beta_2P_2P_1P_2C}),$$

where $B_1 = b_1 - d_{P_1}$, $B_2 = b_2 - d_{P_2}$,

$$S_{sum} = \lambda_{11} + \lambda_{22} - \lambda_{12} - \lambda_{21},$$

$$S_{prod} = \lambda_{11}\lambda_{22} - \lambda_{12}\lambda_{21},$$

$$P_1P_1P_2C = \frac{B_1 - B_2}{S_{sum}} - \frac{d_c h(\lambda_{22} - \lambda_{12})}{S_{sum}(\alpha\gamma - d_c)},$$

$$P_2P_1P_2C = \frac{B_2 - B_1}{S_{sum}} - \frac{d_c h(\lambda_{11} - \lambda_{21})}{S_{sum}(\alpha\gamma - d_c)},$$

$$\text{and } C_{P_1P_2C} = \frac{\gamma h(B_1(\lambda_{22} - \lambda_{21}) - B_2(\lambda_{11} - \lambda_{12}))}{S_{sum}(\alpha\gamma - d_c)} + \frac{\gamma d_c h^2 S_{prod}}{S_{sum}(\alpha\gamma - d_c)^2}$$

- Low food quality coexistence equilibria $(P_1P_2C)_L$:

In this case we assume the $\min(\gamma, \frac{N_1+N_2}{q(P_1+P_2)}) = \frac{N_1+N_2}{q(P_1+P_2)} = \frac{Q_1P_1+Q_2P_2}{q(P_1+P_2)}$. The procedure of finding $(P_1C)_L$ was described in the last section. Similar to the one-producer, one-consumer model, there are up to three equilibria in the two-producer, one-consumer model. The P_1 equilibrium values for $(P_1P_2C)_L$ can be shown to be the roots of a cubic polynomial [7].

Fixing the total nutrient N_T and the second producer growth rate b_2 , a plot of $\frac{Q_1P_1+Q_2P_2}{q(P_1+P_2)}$ at the coexistence equilibria $(P_1P_2C)_H$ and $(P_1P_2C)_L$ against b_1 is shown in figure 5(a). Notation and line types are analogous to those described for figure 2(a). In particular, the bold curves indicate the biomass conversion efficiency on the attractors.

Figures 5(b) and 5(c) are two-parameter bifurcation diagrams for model (4) obtained by varying b_1 and b_2 , but with a fixed $N_T = 0.1$. The solid curves indicate the more significant bifurcations on the attractors, and the dashed curves indicate some of the non-attractor bifurcations. The two-producer, one-consumer coexistence parameter combinations are highlighted in yellow. Figure 5(d) is a bifurcation diagram for the analogous two-producer-one, consumer model without stoichiometry ($\min(\gamma, \frac{Q_1P_1+Q_2P_2}{q(P_1+P_2)}) = \gamma$). The two dashed blue lines forming the wedge shape locate the transcritical bifurcations to two-producer coexistence from a single-producer coexistence when there is no consumer. The red solid curve locate a transcritical bifurcation of periodic orbits: a periodic orbit passes through another periodic orbit in one of the P_iC planes into the interior of the first “octant” of the coordinate plane. The details of bifurcations between

regions are summarized in table 3.

Regions \tilde{A} , \tilde{B} , \tilde{C} , \tilde{D} , \tilde{E} , \tilde{F} , and \tilde{Z} are the “conjugates” of regions A , B , C , D , E , F , and Z , with the roles of P_1 and P_2 interchanged. Thus, the time series in these conjugate regions are not shown. In each time series, solutions of P_1 , P_2 , and C are plotted against the time. Table 3 summarizes the bifurcations between the adjacent regions.

We denote by W the region $(0 \leq b_1 \leq d_{P_1}) \cup (0 \leq b_2 \leq d_{P_2})$. The region is too small to resolve in figures 5(b)-(d). We do not provide time series for region W either; existence of the both producers is not possible here.

5. Experimental Implications

John - fill in here.

- One-producer - can vary b and N_T independently. Two-producers - hard to vary b_1 and b_2 independently.
- Increase light - radial path through b_1 - b_2 space.

6. Conclusions

The model developed and studied in this paper is a simplified model of two producers and one consumer with stoichiometry. It is a generalization of the Rosenzweig and MacArthur model (see (1)), which is a single-producer, single-consumer model without stoichiometry. First, we introduced stoichiometry into Rosenzweig and MacArthur model. This left us with a model similar to the LKE model [8], but with somewhat different mechanisms for effecting stoichiometry. Afterward, we added a second producer.

Following [8], for the single producer model (5) we chose to vary the growth rate, b_1 , and the total nutrient, N_T , both which might be controlled in experiments. As illustrated in figure 3, except for extremely low values of N_T (below approximately 0.2), the model exhibits more than the three bifurcations typically observed in the Rosenzweig and MacArthur model by varying either birth rate or carrying capacity. As the producer's growth rate increases, with a fixed amount of nutrient in the system, there is a sequence of bifurcations: a first transcritical enabling the producer to enter the system, a second transcritical enabling the consumer to enter the system, a Hopf bifurcation creating coexistence limit cycles, a first saddle-node destroying the cycle and replacing it with an attracting equilibrium, a second saddle-node taking the two “extra” saddle coexistence equilibria away, but leaving the attracting coexistence equilibrium, and a transcritical bifurcation after which the consumer can no longer survive. See figures 2(a) and 3(a).

We note that this description is far from a complete analysis of model (5). There are many parameters which we have not varied and which could lead to different behavior. The bifurcation sequence described above differs from the sequence in [8] only by switching the last two bifurcations. Similar models we have studied have the first saddle-node taking place *off* the limit cycle, resulting in a coexisting attracting limit cycle and attracting equilibrium. A later homoclinic destroys the limit cycle and returns the equilibrium to the only attractor. Other scenarios are

likely present in the model as well.

The analysis of the two-producer, one-consumer model (4) provided the most interesting bifurcation scenario (see figures 5(b) and 5(c)). We varied the total nutrient N_T in our numerical experiments, but have presented the two-parameter bifurcation diagram in b_1 and b_2 for only one fixed value of N_T . As in the one-producer model, there are many other parameters which we kept fixed, so the bifurcation scenario we found is again far from a complete analysis of (4). Even with this limitation, however, we have observed new and interesting bifurcations in this two-parameter space. Of special note is the parameter region (colored yellow) in which all three species can coexist. This region is, of course, inside the wedge-shaped region which describes the coexistence region of two producers in the absence of any consumer. Also noteworthy is the existence of transcritical bifurcations of periodic orbits which occur at different parameter values from transcritical bifurcations of equilibria. Sufficiently high growth rates in any direction in the b_1 - b_2 parameter plane results in the extinction of the consumer - the “paradox” of energy enrichment.

To summarize, the introduction of stoichiometry to our producer-consumer model can cause the loss of large amplitude limit cycles. Because the total nutrient N_T is fixed, a sufficiently high growth in producer(s) results in the extinction of the consumer as producer xxx nutrient increases simultaneous to reduce food quality. Adding second competing producer creates additional interesting bifurcations, allowing us to see the somewhat complicated criteria for coexistence of all three species.

Acknowledgements

We thank University of Minnesota for support our project funding.

Table 1. Table of Variables

| Variables | Definitions |
|-------------------------|---|
| P_1 | Population Density of Producer P_1 (Carbon) |
| P_2 | Population Density of Producer P_2 (Carbon) |
| C | Population Density of Consumer C (Carbon) |
| N_1 | Nutrient of Producer P_1 |
| N_2 | Nutrient of Producer P_2 |
| N_C | Nutrient of Consumer C |
| M | Mineralized Nutrient |
| $Q_1 = \frac{N_1}{P_1}$ | Stoichiometric Ratio of P_1 |
| $Q_2 = \frac{N_2}{P_2}$ | Stoichiometric Ratio of P_2 |

Table 2. Bifurcations between the adjacent regions in figure 3(a)

| Regions boundary covering | Type of Bifurcation | Involved Attractors | Non-Attractor Transitions |
|---------------------------|--------------------------|---|---|
| $O \rightarrow A$ | Transcritical | $(O) \rightarrow (P_1)$ | |
| $A \rightarrow B$ | Transcritical | $(P_1) \rightarrow (P_1 C)_H$ | |
| $B \rightarrow C$ | Hopf | $(P_1 C)_H \rightarrow$ limit cycle | |
| $C \rightarrow D$ | Homoclinic / Saddle-node | limit cycle \rightarrow Stable $(P_1 C)_L$ | A second unstable $(P_1 C)_L$ is created. |
| $D \rightarrow E$ | Non-Smooth Saddle-node | Stable $(P_1 C)_L \rightarrow$ Stable $(P_1 C)_L$ | The unstable $(P_1 C)_H$ and unstable $(P_1 C)_L$ are eliminated. |
| $E \rightarrow F$ | Transcritical | $(P_1 C)_L \rightarrow (P_1)$ | |

Table 3. Bifurcations between the adjacent regions in figures 5(b) and 5(c)

| Regions boundary covering | Type of Bifurcation | Involved Attractors | Non-Attractor Transitions |
|---------------------------|--------------------------|---|---|
| $W \rightarrow G$ | Transcritical | $(O) \rightarrow (P_1 P_2)$ | |
| $W \rightarrow A$ | Transcritical | $(O) \rightarrow (P_1)$ | |
| $A \rightarrow G$ | Transcritical | $(P_1) \rightarrow (P_1 P_2)$ | |
| $G \rightarrow H$ | Transcritical | $(P_1 P_2) \rightarrow (P_1 P_2 C)_H$ | |
| $A \rightarrow B$ | Transcritical | $(P_1) \rightarrow (P_1 C)_H$ | |
| $B \rightarrow H$ | Transcritical | $(P_1 C)_H \rightarrow (P_1 P_2 C)_H$ | |
| $H \rightarrow I$ | Hopf | $(P_1 P_2 C)_H \rightarrow$ Interior limit cycle | |
| $B \rightarrow C$ | Hopf | $(P_1 C)_H \rightarrow P_1 C$ planar limit cycle | |
| $C \rightarrow Z$ | Transcritical | Limit cycle in $P_1 C$ plane \rightarrow the interior limit cycle | |
| $Z \rightarrow I$ | Transcritical | | $(P_1 C)_H \rightarrow (P_1 P_2 C)_H$ |
| $I \rightarrow J$ | Saddle-node / Homoclinic | Interior limit cycle \rightarrow Stable $(P_1 P_2 C)_L$ | Unstable $(P_1 P_2 C)_L$ is created. |
| $Z \rightarrow J$ | Saddle-node / Homoclinic | Interior limit cycle \rightarrow Stable $(P_1 P_2 C)_L$ | Unstable $(P_1 P_2 C)_L$ is created. |
| $C \rightarrow D$ | Saddle-node / Homoclinic | $P_1 C$ plane limit cycle \rightarrow Stable $(P_1 C)_L$ | Unstable $(P_1 C)_L$ is created. |
| $D \rightarrow J$ | Transcritical | $(P_1 C)_L \rightarrow (P_1 P_2 C)_L$ | |
| $J \rightarrow K$ | Non-Smooth Saddle-node | | Unstable $(P_1 P_2 C)_H$ and unstable $(P_1 P_2 C)_L$ coalesce. |
| $D \rightarrow E$ | Non-Smooth Saddle-node | Stable $(P_1 C)_L \rightarrow$ Stable $(P_1 C)_L$ | Unstable $(P_1 C)_H$ and unstable $(P_1 C)_L$ coalesce. |
| $E \rightarrow J$ | Transcritical | $(P_1 C)_L \rightarrow (P_1 P_2 C)_L$ | |
| $E \rightarrow K$ | Transcritical | $(P_1 C)_L \rightarrow (P_1 P_2 C)_L$ | |
| $K \rightarrow M$ | Transcritical | $(P_1 P_2 C)_L \rightarrow (P_1 P_2)$ | |
| $E \rightarrow F$ | Transcritical | $(P_1 C)_L \rightarrow (P_1)$ | |
| $F \rightarrow M$ | Transcritical | $(P_1) \rightarrow (P_1 P_2)$ | |

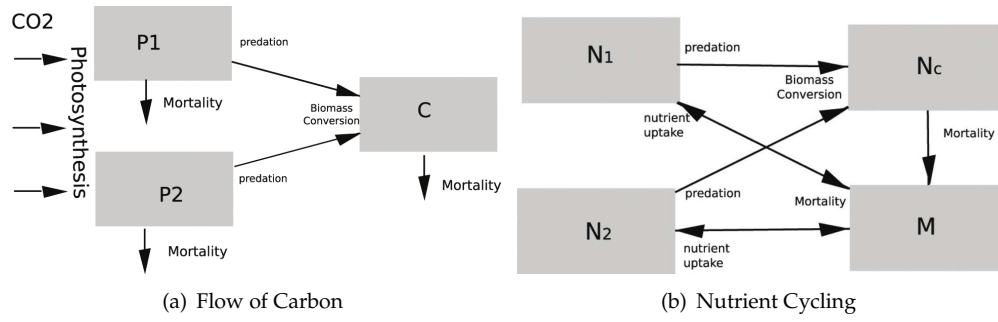


Figure 1. Two-Producer-One-Consumer Flow Charts: Carbon Flow and Nutrient Cycling

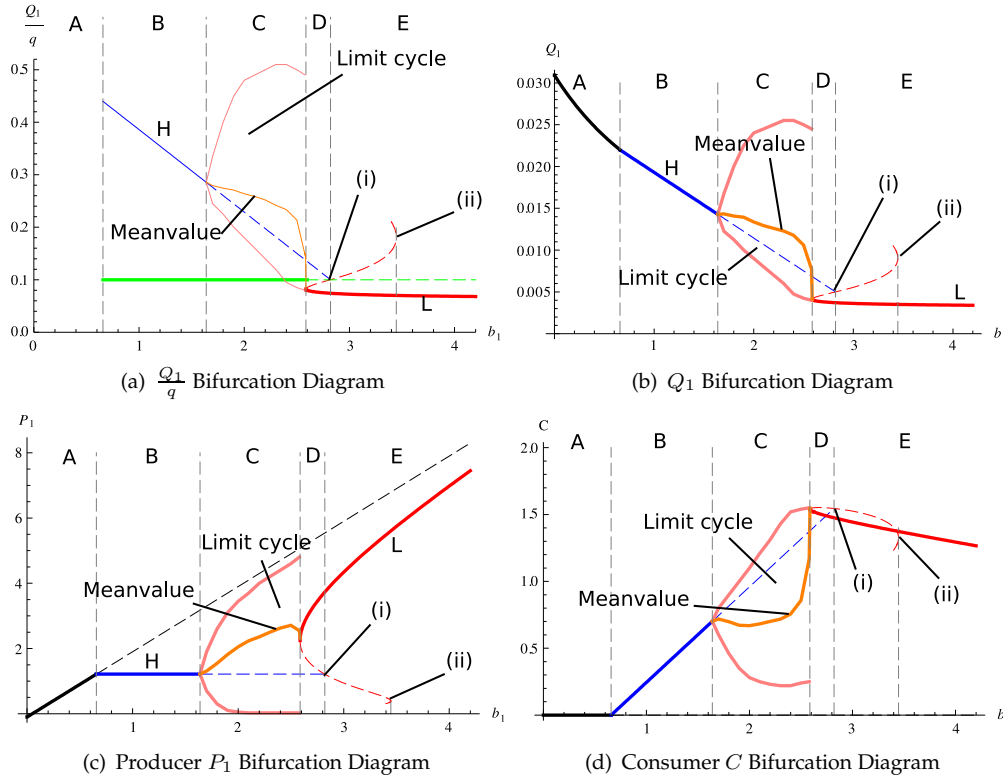


Figure 2. One-parameter bifurcation diagrams for One-Producer-One-Consumer Model. In figures, (i) is a non-smooth saddle-node bifurcation, which is caused by the min function (see table 2). (ii) is a smooth saddle-node bifurcation when two unstable case L equilibria merge. The Meanvalue of a limit cycle is the expected value of (P_1, C, Q_1) from $t = 1000$ to $t = 2000$ with time step 0.01. Regions A, B, C, D, and E are corresponding to figure 3 and the bifurcations between adjacent regions are described in table 2. (a) Plot of $\frac{Q_1}{q}$ at potential equilibria (and range of $\frac{Q_1}{q}$ along periodic orbit in region C). The conversion efficiencies at biologically meaningful equilibria and periodic orbits are in bold. Red corresponds to case L; blue corresponds to case H. Solid indicates stable; dashed indicates unstable. (b) Equilibrium values of Q_1 versus b_1 for equilibrium solutions; range of Q_1 values for periodic orbits in region C. Solid bold lines represent stable equilibria and limit cycle; dashed lines represent unstable equilibria. (See text.) (c) and (d) same as (b) but for P_1 versus b_1 and C versus b_1 .

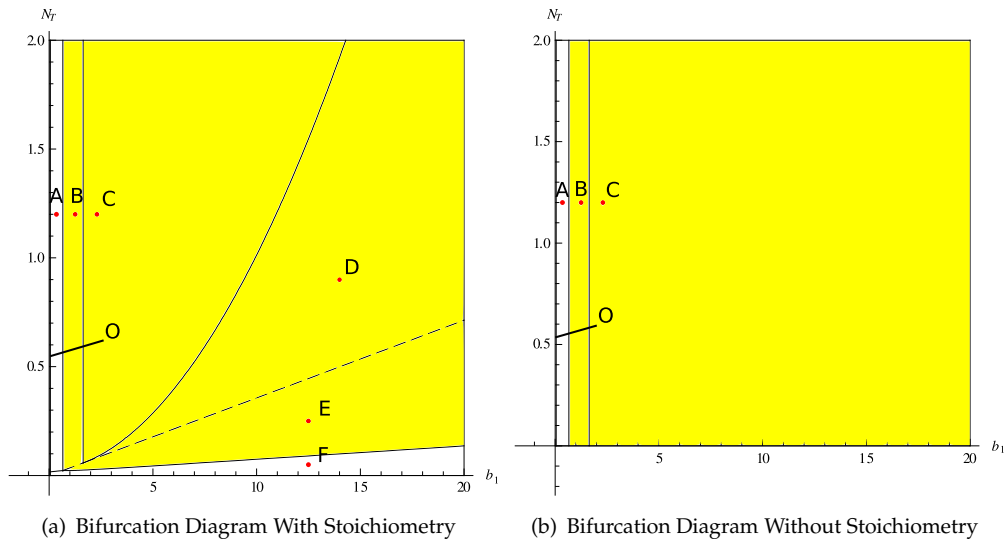


Figure 3. Two-parameter bifurcation diagrams in b and N_T for the One-Producer-One-Consumer Model. Region O is the area of $0 \leq b_1 \leq d_{P_1} = 0.05 \text{ month}^{-1}$. The yellow highlight regions indicate the coexistence of producer and consumer. (a) Two-parameter bifurcation diagram in b_1 and N_T for the One-Producer,One-Consumer Model See figure 4 for representative time series corresponding to each region, and table 2 for bifurcations between adjacent regions. (b) is the two-parameter bifurcation diagram in b_1 and N_T for the corresponding One-Producer,One-Consumer Model without stoichiometry.

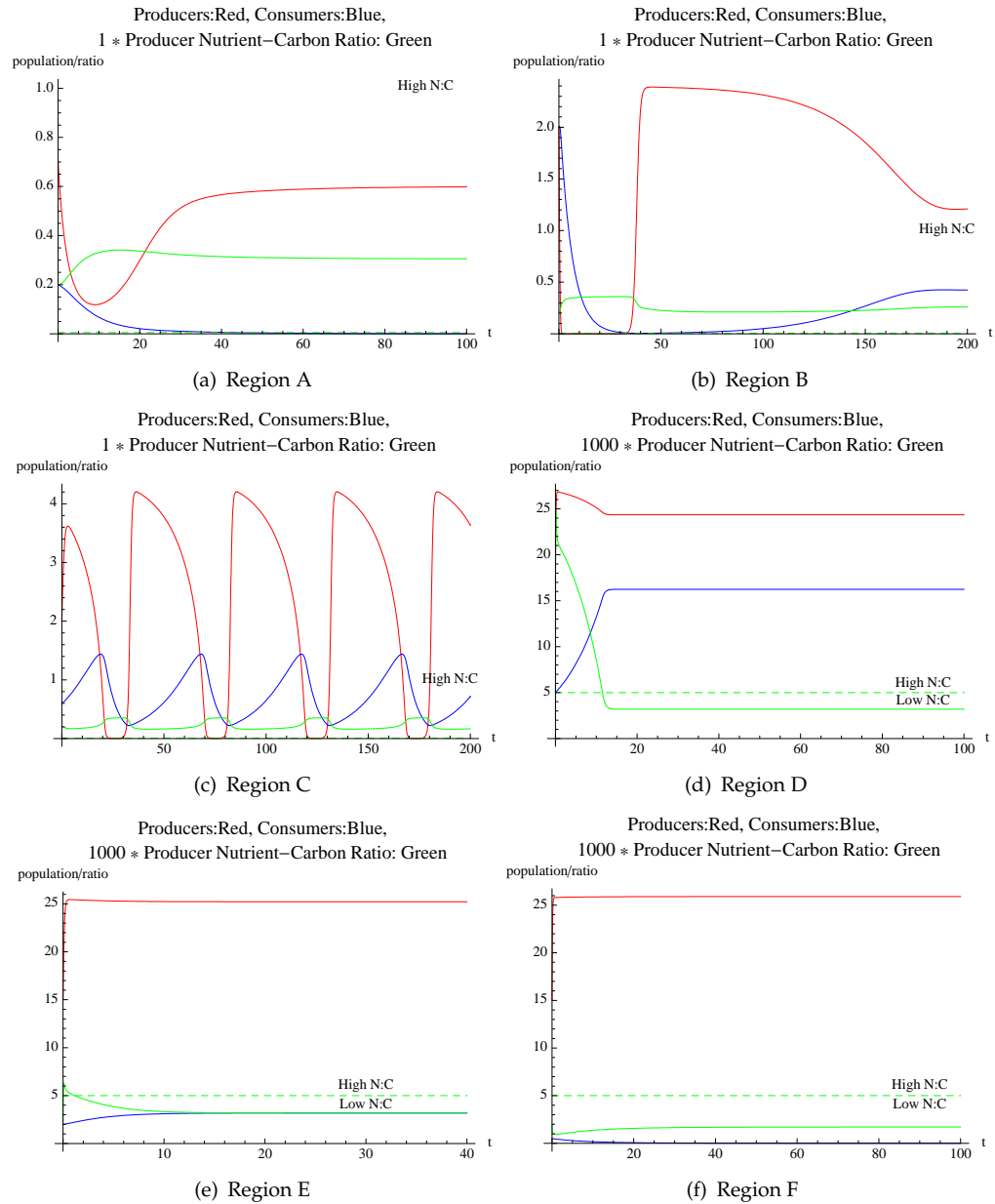


Figure 4. Representative time series corresponding to parameter regions in figure 3. The dashed line is multiplier $\times \gamma q$, which is used as a reference to indicate whether producer's N:C ratio, Q_1 , is relatively high or low to the consumer. When Q_1 is high, consumer's conversion efficiency is γ . Otherwise, the conversion efficiency is $\frac{Q_1}{q}$. Red is for producer; blue is for consumer; green is for producer's N:C ratio.

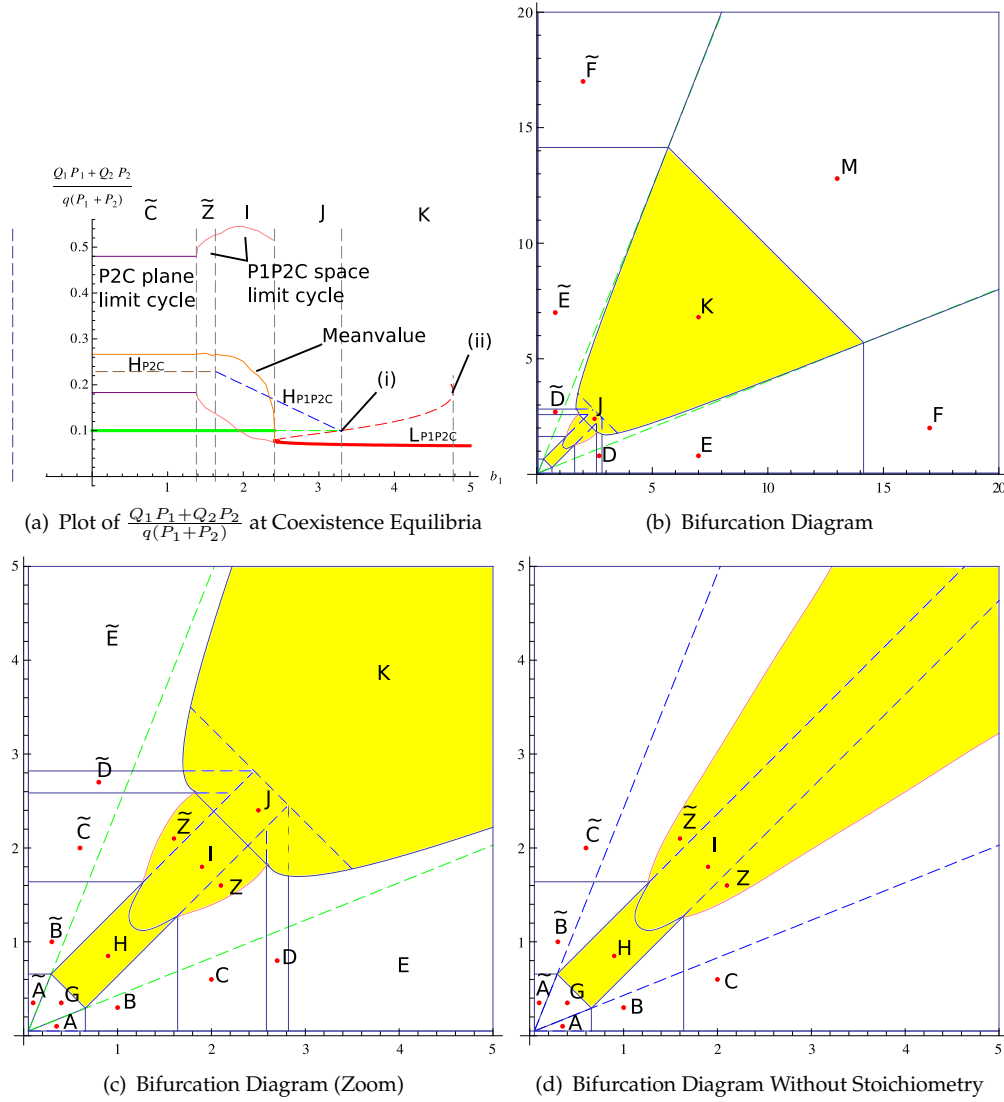


Figure 5. Two-parameter bifurcation diagrams for Two-Producer-One-Consumer Model. The yellow regions in (b), (c), and (d) indicate the coexistence of both producers and consumer. (a) Plot of $\frac{Q_1 P_1 + Q_2 P_2}{q(P_1 + P_2)}$ at potential equilibria, and range of $\frac{Q_1 P_1 + Q_2 P_2}{q(P_1 + P_2)}$ along periodic orbit in region \tilde{Z} and I. The total nutrient N_T and growth rate b_2 are fixed, 0.1 g and 2 month⁻¹. In region \tilde{C} , P_1 is assumed to be zero although initially P_1 can be some positive numbers. It is because population P_1 cannot persist over time in region \tilde{C} . At $b_1 = 0$, the population dynamics of the second producer and the consumer is already forming a limit cycle on P_2C plane. When $b_1 < \sim 1.38$, population of P_1 is unable to persist over time and become extinct or very low in size to have significant influences to the system. Starting from region \tilde{Z} ($b_1 \geq \sim 1.38$), P_1 becomes persistent, which is reflected by the interior limit cycle in P_1P_2C space. The interior limit cycle exists in regions \tilde{Z} and I, and the difference between both cycles in both regions is that there is no corresponding unstable (P_1P_2C) equilibrium in the interior space in region \tilde{Z} , but there is one in region I. Thus, the brown and the blue dashed lines are the $\frac{Q_1 P_1 + Q_2 P_2}{q(P_1 + P_2)}$ at the unstable $(P_2C)_H$ and the unstable $(P_1P_2C)_H$, respectively. The red lines are the $\frac{Q_1 P_1 + Q_2 P_2}{q(P_1 + P_2)}$ at $(P_1P_2C)_L$ equilibria. Solid indicates stable; dashed indicates unstable. The conversion efficiencies of biologically meaningful equilibria and periodic orbits is in bold. The Meanvalue of a limit cycle is the expected value of (P_1, P_2, C, Q_1, Q_2) from $t = 1000$ to $t = 2000$ with time step 0.01. (b) and (c) Two-parameter bifurcation diagrams in b_1 and b_2 for the Two-Producer,One-Consumer Model. See figure 4 for representative time series corresponding to each region, and table 3 for bifurcations between adjacent regions. (d) is the two-parameter bifurcation diagram in b_1 and b_2 for the corresponding Two-Producer,One-Consumer Model without stoichiometry.

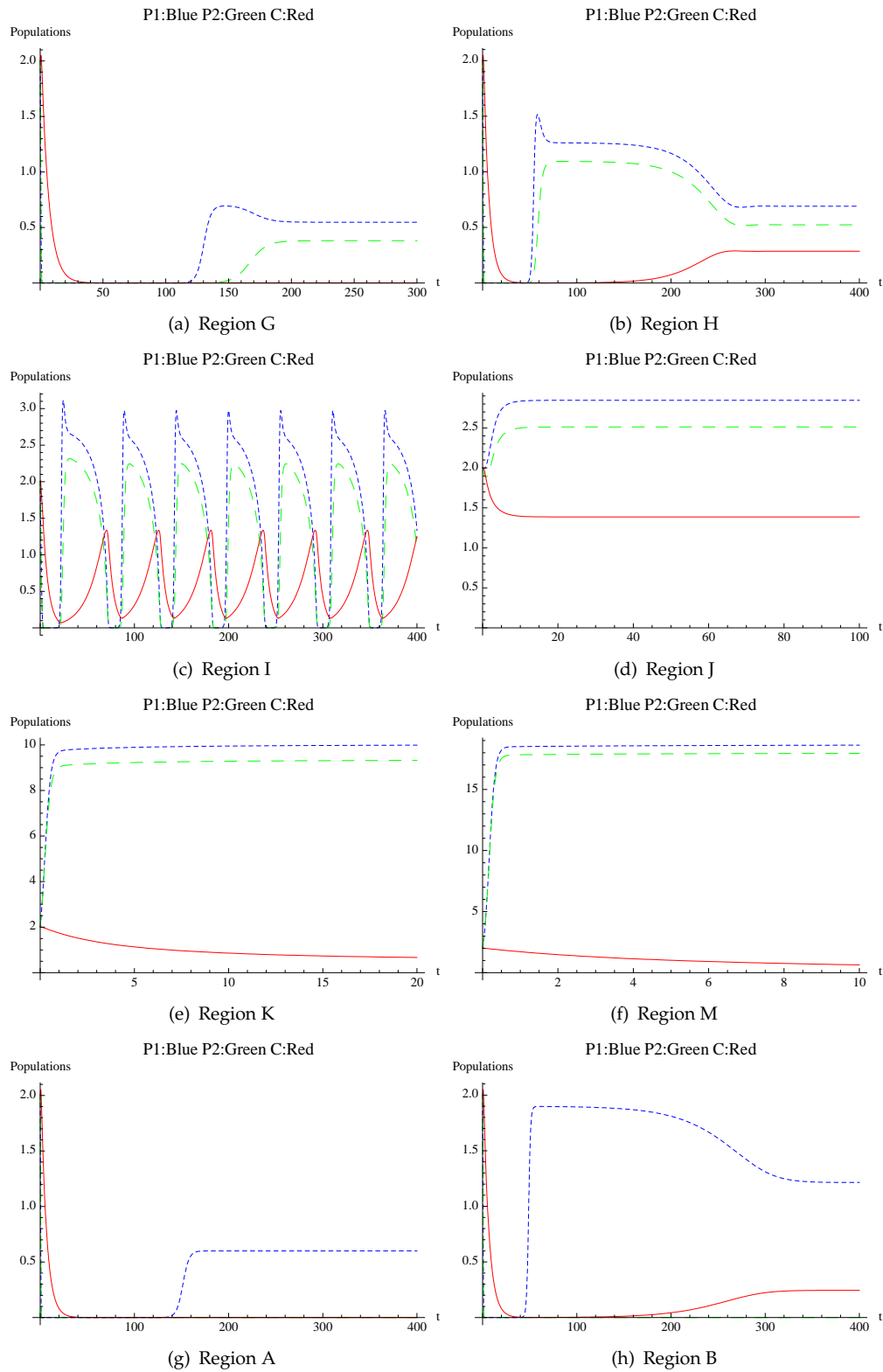


Figure 6. Representative time series corresponding to parameter regions in figure 5. Red is for the consumer; blue is for producer P_1 ; Green is for producer P_2 .

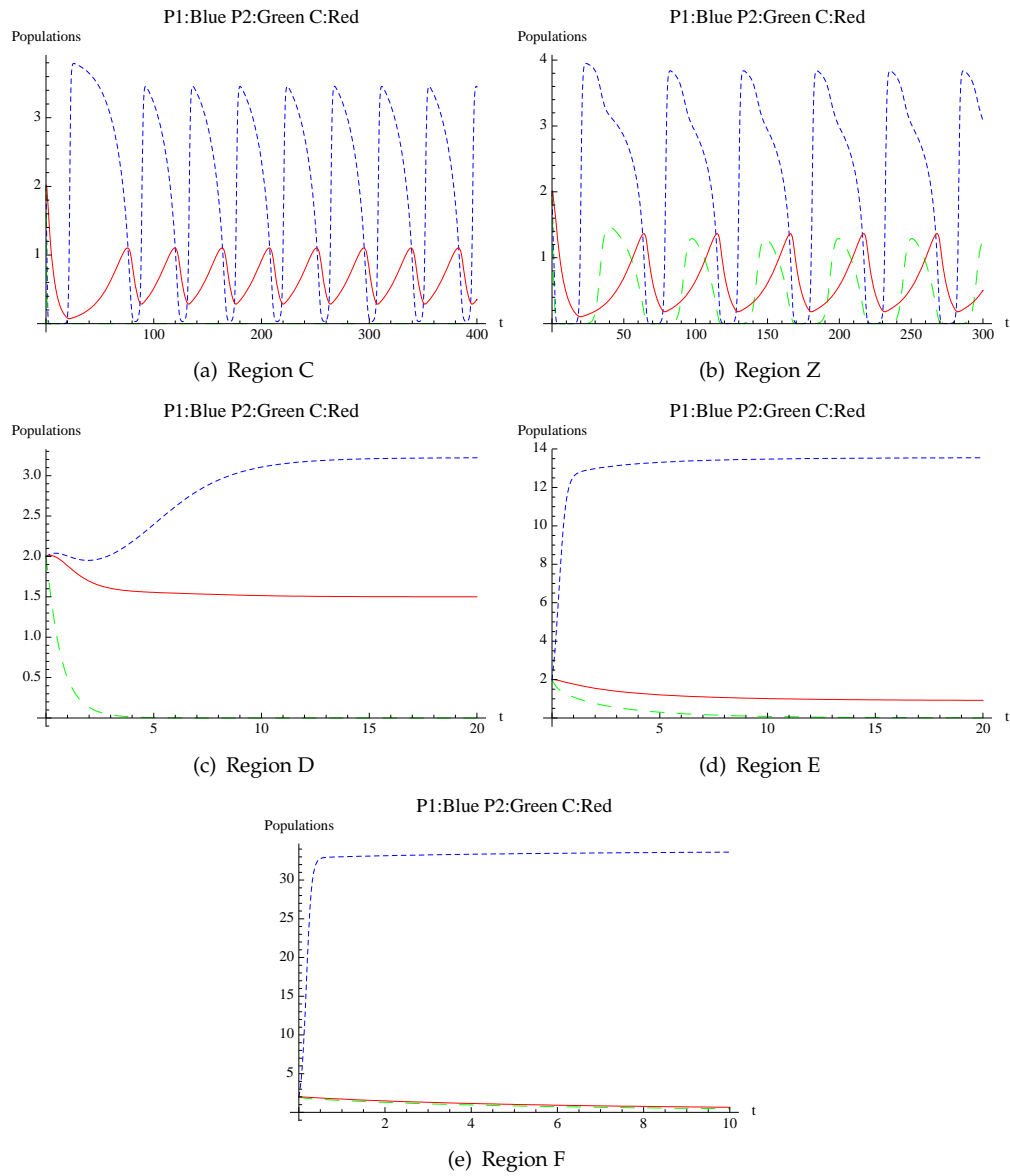


Figure 7. Representative time series corresponding to parameter regions in figure 5. Red is for the consumer; blue is for producer P_1 ; Green is for producer P_2 .

References

- [1] T. Anderson, J. Elser, and D.O. Hessen, *Stoichiometry and population dynamics*, Bulletin of Mathematical Biology 7 (2004), pp. 884–900.
- [2] F.J. Ayala, M.E. Gilpin, and J.G. Ehrenfield, *Competition between species: theoretical models and experimental tests*, Theoretical Population Biology 4 (1973), pp. 331–356.
- [3] A. Cates, *A mathematical investigation of the decomposition of leaf litter*, Master's thesis, University of Minnesota Duluth (2000), supervised by Stech H.S.
- [4] S. Diehl, *Paradoxes of enrichment: Effects of increased light versus nutrient supply on pelagic producer-grazer systems*, The American Naturalist 169 (2007).
- [5] M. Fan, I. Loladze, K. Yang, and J. Elser, *Dynamics of a stoichiometric discrete producer-grazer model*, Journal of Difference Equations and Applications 11 (2005), pp. 347–365.
- [6] Y. Kuang, J. Huisman, and J. Elser, *Stoichiometric plant-herbivore models and their interpretation*, Mathematical Biosciences and Engineering 1 (2004), pp. 215–222.
- [7] L. Lin, *A stoichiometric model of two producers and one consumer*, Master's thesis, University of Minnesota Duluth (2008), supervised by Peckham B B, Pastor J, and Stech H S.
- [8] I. Loladze, Y. Kuang, and J. Elser, *Stoichiometry in producer-grazer systems: Linking energy flow with element cycling*, Bulletin of Mathematical Biology 62 (2000), pp. 1137–1162.
- [9] I. Loladze, Y. Kuang, J. Elser, and W. Fagan, *Competition and stoichiometry: Coexistence of two predators on one prey*, Theoretical Population Biology 65 (2004), pp. 1–15.
- [10] J. Pastor and Y. Cohen, *Herbivores, the functional diversity of plants, and cycling of nutrients in ecosystems*, Theoretical Population Biology 51 (1997), pp. 165–179.
- [11] M.L. Rosenzweig and R.H. MacArthur, *Graphical representation and stability conditions for predator-prey interactions*, American Naturalist 97 (1963), pp. 209–223.
- [12] R. Sterner and J. Elser, *Ecological Stoichiometry*, Princeton University Press (2002).
- [13] G. Sui, M. Fan, I. Loladze, and K. Yang, *The dynamics of a stoichiometric plant-herbivore model and its discrete analog*, Mathematical Biosciences and Engineering 4 (2007), pp. 1–18.
- [14] J. Urabe and R. Sterner, *Regulation of herbivore growth by the balance of light and nutrients*, Proceeding of the National Academy of Sciences of the United States of America 93 (1996), pp. 8465–8469.
- [15] H. Wang, Y. Kuang, and I. Loladze, *Dynamics of a mechanistically derived stoichiometric producer-grazer model*, Journal of Biological Dynamics 00 (2007), pp. 1–11.
- [16] L. Zimmermann, *A producer-consumer model with stoichiometry*, Master's thesis, University of Minnesota Duluth (2006), supervised by Peckham B B, Pastor J, and Stech H S.